Original Article

Magnetohydrodynamic flow of dusty fluid over Riga plate with deforming isothermal surfaces with convective boundary condition

B.C. Prasannakumara[1], N.S. Shashikumar[2], and Gosikere Kenchappa Ramesh[3*]

[1] *Department of Mathematics, Davangere University, Davangere, Karnataka, 577002 India*

[2] *Department of P.G. Studies and Research in Mathematics, Kuvempu University, Shimoga, Karnataka, 577451 India*

[3] *Department of Mathematics, KLE'S J.T. College, Gadag, Karnataka, 582101 India*

Abstract

The present study investigates the flow problem of MHD viscous two-phase dusty flow and heat transfer over a permeable stretching isothermal Riga plate embedded in a porous medium in the presence of convective boundary condition. The wall boundary is subjected to a linear deformation as well as to a quadratic surface temperature. The governing partial differential equations are transformed into ordinary differential equations using similarity variables, which are solved by numerically using fourth order Runge-Kutta method with shooting technique. The impact of various pertinent parameters for the velocity and temperature fields are profiles are analyzed in detail through graphs. Also, friction factor and Nusselt numbers are discussed and presented through tables. The output reveals that higher values of permeability decelerate the velocity and accelerate the temperature profile of both phases and it is noted that the velocity phase is always larger than the dust phase.

Keywords: dusty fluid, Riga plate, convective boundary condition, stretching sheet, numerical solutions

1. Introduction

In nature, the fluid fit as a fiddle is every now and then open. Water and air contain degradations like clean particles and remote bodies. As of late, pros have swung to focus dusty fluid. Examination of reason for control layer stream and warmth move in dusty fluid is to an unprecedented degree essential in understanding and depending the various mechanical and depicting issues stressed over trademark fallout, powder progress, rain crumbling in guided rockets, sedimentation, start, fluidization, nuclear reactor cooling, electrostatic precipitation of spotless, misuse water treatment, acoustics group settling, luner super hot remains streams vaporized and paint sprinkling, and so forth. In recent decades, pros have been focusing on separating the sparkle and mass trade characteristics of dusty fluid through different channels. Fundamental studies in dynamics of dusty fluid, its behavior and boundary layer modeling have been initiated by Saffman (1962). Based on the above applications Chakrabarti (1974) analyzed the boundary layer flow of a dusty gas. Datta, & Mishra (1982) have investigated boundary layer flow of a dusty fluid over a semi-infinite flat plate. Vajravelu, & Nayfeh (1992) investigated hydromagnetic flow of a dusty fluid over a porous stretching sheet. Gireesha, Ramesh, Abel, & Bagewadi (2011) described the boundary layer flow and heat transfer analysis of dusty fluid past a stretching sheet in the presence of non-uniform heat source/sink. The effect of temperature-dependent thermal conductivity and viscosity on unsteady MHD Couette flow and heat transfer of viscous dusty fluid between two parallel plates has been investigated by Mosayebidorcheh, Hatami, Ganji, Mosayebidorcheh, & Mirmohammadsadeghi (2015). Prakash, Makinde, Kumar, & Dwivedi, (2015) examined the combined effects of thermal radiation, buoyancy force and magnetic field on heat transfer on MHD oscillatory dusty fluid flow through a vertical channel filled with a porous medium. Ahmed, Khan, &

Mohyud-Din (2017b) analyzed the impact of nonlinear thermal radiation on the viscous flow through a porous channel. The steady two-dimensional, incompressible, laminar boundary layer flow and heat transfer of a dusty fluid towards a stretching sheet was investigated by Ramesh, & Gireesha (2013) using similarity solution approach. Turkyilmazoglu (2017) discussed the magnetohydrodynamic flow of a viscous two-phase dusty fluid and heat transfer over permeable (Gireesha, Venkatesh, Shashikumar, & Prasanna kumara, 2017) implemented (Saffman, 1962) model to investigate the effect of thermal stratification on MHD flow and heat transfer of dusty fluid over a vertical stretching sheet embedded in a thermally stratified porous medium in the presence of uniform heat source and thermal radiation. Bhatti, & Zeeshan (2017) examined the peristaltic motion of a fluid particle suspension with the effect of slip. Recently, Ramesh, Chamkha, & Gireesha (2016); Hamid, Nazar, & Pop (2017); and Ramesh, Gireesha, & Gorla (2015, 2015b) numerically studied the boundary layer flow of dusty fluid through different geometries.

The flow-control device of Gailitis and Lielausis is an electromagnetic actuator which consists of a spanwise aligned array of alternating electrodes and permanent magnets, mounted on a plane surface as seen in Figure 1. This set-up, sometimes is a Riga-plate, can be applied to reduce the friction and pressure drag of submarines by preventing boundary-layer separation as well as by diminishing turbulence production. Initially, Gailitis, & Lielausis (1961) introduced a flow control device called a Riga plate. Ahmad, Asghar, & Afzal (2016) examined the mixed convection boundary layer flow of a nanofluid past a vertical Riga plate in the presence of strong suction. Hayat, Abbas, Ayub, Farooq, & Alsaedi (2016) presented a computational modeling to analyze the effect of heat generation/absorption on the boundary layer flow of a nano fluid induced by a variable thickness Riga plate with convective boundary condition. The boundary layer flows of electro magneto hydrodynamic on nanofluid over a Riga plate with slip effect have been analyzed by Ayub, Abbas, & Bhatti (2016). The simultaneous effects of thermal radiation and EMHD on viscous nanofluid flow through a horizontal Riga plate have been analyzed by Bhatti, Abbas, & Rashidi (2016). Entropy generation on viscous nanofluid with mixed convection boundary layer flow induced by a horizontal Riga plate has been examined by Abbas, Ayub, Bhatti, Rashidi, & El-Sayed, Ali (2016). Farooq, Anjum, Hayat, & Alsaedi (2016) discussed the phenomenon of melting heat transfer in boundary layer stagnation point flow of viscous fluid towards a Riga plate of variable thickness. A substantial number of experimental and theoretical studies have been carried out by numerous researchers on Riga plate (Iqbal, Mehmood, Azhar, & Maraj, 2017; Ahmed, Khan, & Mohyud-Din, 2017a; Ramesh & Gireesha, 2017a; Ramesh, Roopa, Gireesha, Shehzad, & Abbasi, 2017b; Abbas, Hayat, Ayub, Bhatti, & Alsaedi, 2017a; Abbas, Bhatti, & Ayub, 2017b). Recently, Hayat, Khan, Imtiaz, & Alsaedi (2017) explored the structure of convective heat transfer of electro magneto hydrodynamic squeezed flow past a Riga plate.

The principal inspiration of the issue is to examine the limit layer flow of two-stage dusty fluid show over a Riga-plate through a peaceful incompressible thick electrically leading dusty liquid implanted in a permeable medium.

Convective point of confinement condition is for the most part used to describe a direct convective heat exchange condition for no less than one scientific component in heat. The representing conditions are changed into non-straight standard differential condition by utilizing similitude change and
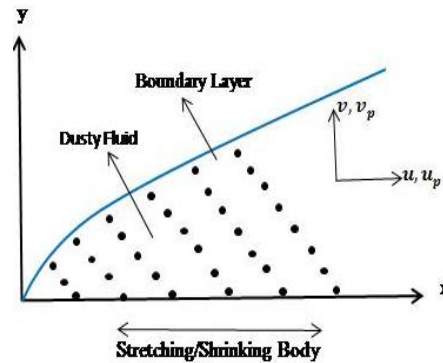

Figure 1.   Schematic representation of the flow diagram.

afterward fathomed numerically utilizing Runge-Kutta-Fehlberg-45 arrange strategy with shooting procedure. The practices of each of the non-dimensional amounts are uncovered graphically for all the liquid parameters. Additionally, contact factor and Nusselt numbers are described and displayed through charts.

2. Formulation

Consider a steady two-dimensional motion of laminar boundary layer flow of an incompressible viscous electrically conducting dusty fluid over a permeable stretching isothermal Riga plate with variable thickness embedded in a porous medium as seen in Figure 1 and Figure 2. The stretching coincides with the plane $y = 0$. It is assumed that the velocity of the sheet is linear, that is $u_w(x) = cx$, with $c > 0$ for a stretching sheet. It is also assumed that the local temperature of the sheet is T_w, while that of the ambient fluid and dust particles is T_∞. The porous medium is assumed to be transparent and in thermal equilibrium with the fluid. The particles are taken to be small enough and of sufficient number and are treated as a continuum which allow concepts such as density and velocity to have physical meaning. A uniform magnetic field B_0 is applied in the transverse direction $y > 0$ normal to the plate. The dust particles are assumed to be spherical in shape, uniform in size and possessing constant number density.
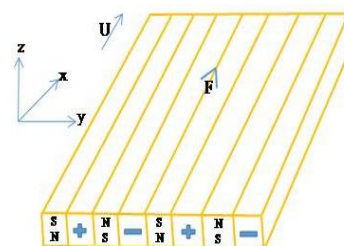

Figure 2.   Riga plate.

Under these assumptions, along with the usual boundary layer approximations, the governing equations for the flow are,

$$\frac{\partial u}{\partial x} + \frac{\partial v}{\partial y} = 0, \tag{1}$$

$$u\frac{\partial u}{\partial x} + v\frac{\partial u}{\partial y} = \nu\frac{\partial^2 u}{\partial y^2} + \frac{KN}{\rho}(u_p - u) - \frac{\nu}{k_p}u + \frac{\pi j_0 M_0}{8\rho}\exp\left(-\frac{\pi}{a}y\right), \tag{2}$$

$$\frac{\partial u_p}{\partial x} + \frac{\partial v_p}{\partial y} = 0, \tag{3}$$

$$u_p\frac{\partial u_p}{\partial x} + v_p\frac{\partial u_p}{\partial y} = \frac{K}{m}(u - u_p), \tag{4}$$

$$\rho c_p\left(u\frac{\partial T}{\partial x} + v\frac{\partial T}{\partial y}\right) = k\frac{\partial^2 T}{\partial y^2} + \frac{\rho_p c_m}{\tau_T}(T_p - T) + \frac{\rho_p}{\tau_v}(u_p - u)^2 - \frac{\partial q_r}{\partial y}, \tag{5}$$

$$\rho_p c_m\left(u_p\frac{\partial T_p}{\partial x} + v_p\frac{\partial T_p}{\partial y}\right) = \frac{\rho_p c_m}{\tau_T}(T_p - T), \tag{6}$$

with the boundary conditions

$$u = U_w(x) = cx, v = 0, -k\frac{\partial T}{\partial y} = h_f(T_w - T) \text{ at } y = 0,$$

$$u \to 0, u_p \to 0, v_p \to v, \ T \to T_\infty, T_p \to T_\infty \text{ as } y \to \infty, \tag{7}$$

where (u, v) and (u_p, v_p) are the velocity components of the fluid and dust particle phases along x and y directions respectively. ν, K, N, ρ are the kinematic viscosity of the fluid, Stokes resistance or drag coefficient, number of dust particle per unit volume, density of the fluid, respectively. k_p is the permeability of the porous medium, j_0 is the applied current density in the electrodes, M_0 is the magnetization of the permanent magnets mounted on the surface of the Riga plate, a denotes the width of the magnets between the electrodes, m is the mass of the dust particle. T and T_p are the temperature of the fluid and temperature of the dust particle respectively, c_p and c_m are the specific heat of fluid and dust particles, τ_T is the thermal equilibrium time i.e., the time required by the dust cloud to adjust its temperature to the fluid, τ_v is the relaxation time of the of dust particle i.e., the time required for a dust particle to adjust its velocity relative to the fluid. Further, b is a constant with $b > 0$ for a heated plate $(T_w > T_\infty)$ and $b < 0$ for a cooled surface $(T_w < T_\infty)$, It should be noted that the rest of the momentum equations regarding the fluid and dust particles, which are not cited in "Equation (1)", can be made by evaluating the pressures acting upon the fluid and dust, which is a trivial task, so omitted here.

Using the Rosseland approximation for radiation, radiation heat flux is given by

$$q_r = -\frac{4\sigma^*}{3k^*}\frac{\partial T^4}{\partial y} = -\frac{16\sigma^*}{3k^*}T_\infty^3\frac{\partial T}{\partial y}. \tag{8}$$

where σ^* is the Stefan–Boltzmann constant and k^* is the mean absorption coefficient. Assuming that the temperature differences within the flow such that the term T^4 may be expressed as a linear function of the temperature, and expanding T^4 in a Taylor series about T_∞ and neglecting the higher order terms beyond the first degree in $(T - T_\infty)$, then we get

$$T^4 \cong 4T_\infty^3 T - 3T_\infty^4.$$

Here the energy equation takes the form as follows

$$\rho c_p\left(u\frac{\partial T}{\partial x} + v\frac{\partial T}{\partial y}\right) = \frac{\partial}{\partial y}\left[\left(k + \frac{16\sigma^* T_\infty^3}{3k^*}\right)\frac{\partial T}{\partial y}\right] + \frac{\rho_p c_m}{\tau_T}(T_p - T) + \frac{\rho_p}{\tau_v}(u_p - u)^2. \tag{9}$$

The mathematical analysis of the current physical problem is simplified by introducing the subsequent similarity transformations based on the dimensionless boundary layer co-ordinate η,

$$u = cxf'(\eta), \; v = -\sqrt{cv}\, f(\eta), \; \eta = \sqrt{\frac{c}{v}}y, u_p = cxF'(\eta),$$

$$v_p = -\sqrt{cv}F(\eta), \quad \theta(\eta) = \frac{T-T_\infty}{T_w-T_\infty}, \; \theta_p(\eta) = \frac{T_p-T_\infty}{T_w-T_\infty}, T_w - T_\infty > 0 \tag{10}$$

where T_w and T_∞ denote the temperature at the wall and at large distance from the wall, respectively. The governing equations of motion for the two-phase fluid flow and heat transfer "Equation (2)", "Equation (4)", "Equation (6)" and "Equation (9)" are then reduced to

$$f''' + f f'' - (f')^2 + l\beta[F' - f'] - Sf' + Q\exp(-A\eta) = 0, \tag{11}$$

$$F'^2 - F F'' + \beta[F' - f'] = 0, \tag{12}$$

$$\left(1+\frac{4Rd}{3}\right)\theta'' + \Pr[f\,\theta' - 2f'\theta] + \Pr l\gamma\beta_T\big(\theta_p - \theta\big) + l\beta\Pr Ec(F' - f')^2 = 0, \tag{13}$$

$$2\,F'\theta_p - F\theta'_p + \beta_T\big(\theta_p - \theta\big) = 0, \tag{14}$$

The corresponding boundary conditions will take the following form,

$$f(\eta) = 0, f'(\eta) = 1, \theta'(\eta) = -B_i(1 - \theta(\eta)) \text{ at } \eta = 0,$$

$$f'(\eta) \to 0, F'(\eta) \to 0, F(\eta) \to f(\eta), \theta(\eta) \to 0, \theta_p(\eta) \to 0 \text{ as } \eta \to \infty \tag{15}$$

where $l = \frac{\rho_p}{\rho}$ is the mass concentration of dust particles (or particle loading parameter) with $\rho_p = Nm$, standing for the density of the particle phase, $\beta = \frac{1}{c\tau_v}$, is the fluid particle interaction parameter for velocity, $S = \frac{v}{k_p c}$ is the permeability parameter, $Rd = \frac{16\sigma^* T_\infty^3}{3kk^*}$ is the radiation parameter, $Q = \frac{\pi j_0 M_0}{8\rho c^2 x}$ is the modified Hartman number, $A = \frac{\pi/a}{c/v}$ is the dimensionless parameter, $Pr = \frac{v\rho c_p}{k}$ is the Prandtl number, $\gamma = \frac{c_m}{c_p}$ is the specific heat parameter, $\beta_T = \frac{1}{c\tau_T}$ is the fluid-interaction parameter for temperature, $Ec = \frac{u_w}{(T_w - T_\infty)c_p}$ is the Eckert number and $B_i = \sqrt{\frac{v}{c}}\frac{h_f}{k}$ is the Biot number.

The physical quantities of interest are the skin friction coefficient C_f and the local Nusselt Number Nu, which are defined as

$$C_{fx} = \frac{\tau_w}{\rho U_w^2}, \qquad Nu = \frac{xq_w}{k(T_w - T_\infty)} \tag{16}$$

where the surface shear stress τ_w and the surface heat flux q_w are given by

$$\tau_w = -\mu\left(\frac{\partial u}{\partial y}\right)_{y=0}, q_w = -k\left(\frac{\partial T}{\partial y}\right)_{y=0} + (q_r)_w. \tag{17}$$

Using the non-dimensional variables, we obtain

$$C_{fx}Re_x^{\frac{1}{2}} = -f''(0), NuRe_x^{-\frac{1}{2}} = -\left(1+\frac{4Rd}{3}\right)\theta'(0). \tag{18}$$

Table 1.   Validation results for the local Nusselt Number $-\theta'(0)$, in the case of $\beta, S, Q, A, \beta_T, Ec$ and Bi.

A	Bi	Ec	kp	Pr	Q	Rd	β	β_T	l	$-f''(0)$	$-\theta'(0)$
0.2	0.5	0.1	2.0	3.0	0.1	1.5	0.5	0.5	1.0	1.771644	0.377063
1.0	0.5	0.1	2.0	3.0	0.1	1.5	0.5	0.5	1.0	1.789484	0.376044
1.8	0.5	0.1	2.0	3.0	0.1	1.5	0.5	0.5	1.0	1.798164	0.375704
0.6	**0.0**	0.1	2.0	3.0	0.1	1.5	0.5	0.5	1.0	1.782444	0
0.6	**1.0**	0.1	2.0	3.0	0.1	1.5	0.5	0.5	1.0	1.782444	0.605168
0.6	**1.5**	0.1	2.0	3.0	0.1	1.5	0.5	0.5	1.0	1.782444	0.758917
0.6	0.5	**0.5**	2.0	3.0	0.1	1.5	0.5	0.5	1.0	1.782444	0.369923
0.6	0.5	**1.0**	2.0	3.0	0.1	1.5	0.5	0.5	1.0	1.782444	0.361825
0.6	0.5	**1.5**	2.0	3.0	0.1	1.5	0.5	0.5	1.0	1.782444	0.353727
0.6	0.5	0.1	**1.5**	3.0	0.1	1.5	0.5	0.5	1.0	1.63702	0.378488
0.6	0.5	0.1	**2.5**	3.0	0.1	1.5	0.5	0.5	1.0	1.917005	0.374419
0.6	0.5	0.1	**3.0**	3.0	0.1	1.5	0.5	0.5	1.0	2.042809	0.372525
0.6	0.5	0.1	2.0	**4.0**	0.1	1.5	0.5	0.5	1.0	1.782444	0.392172
0.6	0.5	0.1	2.0	**5.0**	0.1	1.5	0.5	0.5	1.0	1.782444	0.403032
0.6	0.5	0.1	2.0	**6.0**	0.1	1.5	0.5	0.5	1.0	1.782444	0.411077
0.6	0.5	0.1	2.0	3.0	**0.4**	1.5	0.5	0.5	1.0	1.653821	0.379178
0.6	0.5	0.1	2.0	3.0	**0.8**	1.5	0.5	0.5	1.0	1.484757	0.382045
0.6	0.5	0.1	2.0	3.0	**1.2**	1.5	0.5	0.5	1.0	1.318002	0.384326
0.6	0.5	0.1	2.0	3.0	0.1	**1.0**	0.5	0.5	1.0	1.782444	0.387269
0.6	0.5	0.1	2.0	3.0	0.1	**2.0**	0.5	0.5	1.0	1.782444	0.366583
0.6	0.5	0.1	2.0	3.0	0.1	**2.5**	0.5	0.5	1.0	1.782444	0.357624
0.6	0.5	0.1	2.0	3.0	0.1	1.5	**1.0**	0.5	1.0	1.82808	0.37577
0.6	0.5	0.1	2.0	3.0	0.1	1.5	**2.0**	0.5	1.0	1.872636	0.375567
0.6	0.5	0.1	2.0	3.0	0.1	1.5	**3.0**	0.5	1.0	1.894503	0.37562
0.6	0.5	0.1	2.0	3.0	0.1	1.5	0.5	**1.0**	1.0	1.782444	0.37967
0.6	0.5	0.1	2.0	3.0	0.1	1.5	0.5	**2.0**	1.0	1.782444	0.382884
0.6	0.5	0.1	2.0	3.0	0.1	1.5	0.5	**3.0**	1.0	1.782444	0.384525
0.6	0.5	0.1	2.0	3.0	0.1	1.5	0.5	0.5	**0.5**	1.735576	0.374295
0.6	0.5	0.1	2.0	3.0	0.1	1.5	0.5	0.5	**1.5**	1.828128	0.378363
0.6	0.5	0.1	2.0	3.0	0.1	1.5	0.5	0.5	**2.0**	1.872713	0.380197

3. Numerical Procedure

Equations (11)–(14) are highly non-linear ordinary differential equations. To solve these equations we adopted Runge-Kutta Fehlberg fourth–fifth order method (RKF45 Method) along with shooting method. With the help of shooting technique, missed initial conditions are obtained by converting the boundary value problem into an initial value problem. We have considered infinity condition at a large but finite value of η where negligible variation in velocity and temperature profiles occurs. For the present problem, we took step size $\Delta\eta = 0.001$, $\eta_\infty = 5$ and accuracy to the fifth decimal place. The CPU running-time for existing numerical solution is 0.03 sec. Table 2 presents the validation of present problem made with Grubka, & Bobba (1985) and Chen (1998). It demonstrates an excellent comparison and gives confidence that present numerical technique is accurate.

4. Result and Discussion

Numerical computation has been carried out in order to study the influence of different parameters that describes the flow and heat transfer characteristics of dusty fluid. The results are presented and discussed in detail through graphs. In all figures, the values of the fixed parameters are

$$kp = 2.0, Ec = 0.1, \Pr = 3.0, Q = 0.1, A = 0.6, Rd = 1.5, \beta = \beta_T = 0.5, l = 1.0, B_i = 0.5.$$

Figures 3 and 4 depicts the effect of permeability parameter kp on the velociy and temperature distributions. It is obvious that the presence of porous medium causes higher restriction to the fluid flow, which causes the fluid to decelerate. Therefore, an increase in impermeability parameter causes increased the resistance to the fluid motion and hence velocity decreases of both the phases. The effect of increasing values of permeable parameter contributes to the thickening of the thermal boundary layer, which is shown in Figure 4. This is evident from the fact that the porous medium opposes the fluid motion. The resistance offered to the flow is responsible for enhancing the temperature. Figure 5 shows the behavior of fluid particle interaction parameter of velocity (β) on the velocity distribution. From these figures we observed that the fluid phase velocity decreases and the dust phase velocity increases for increasing the values of β, as shown in Figure 5. It is observed that an increase in fluid-particle interaction parameter, the thickness of momentum boundary layer decreases for fluid phase and this phenomena is opposite for the dust phase. The effect of fluid particle interaction parameter of temperature β_τ on fluid and dust phase temperature profiles are shown in Figure 6. It can be seen that fluid phase temperature decreases and dust phase temperature increases with increase in β_T.
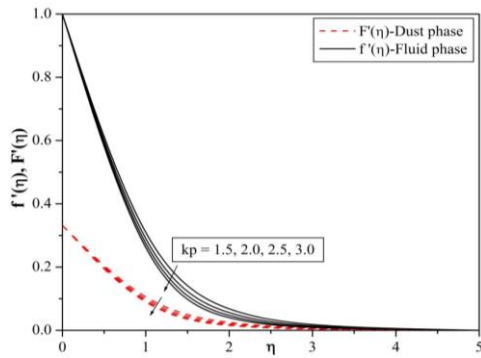
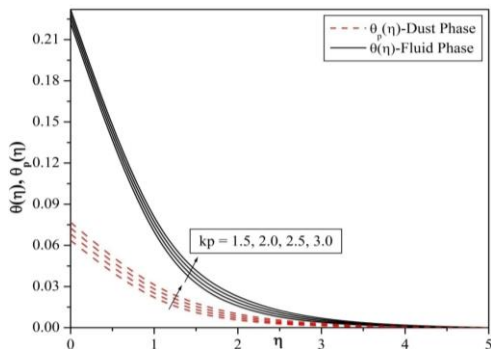Figure 3.   Effect of permeability parameter kp on velocity profile.

Figure 4.   Effect of permeability parameter kp on temperature profile.
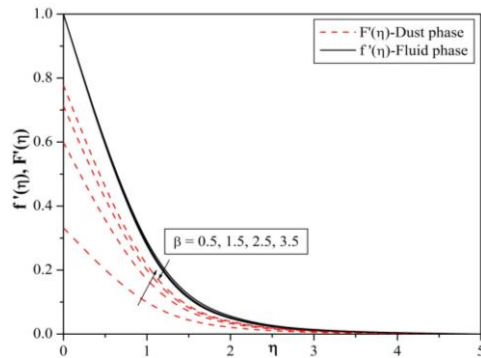

Figure 5.   Effect of fluid particle interaction parameter for velocity β on velocity profile.
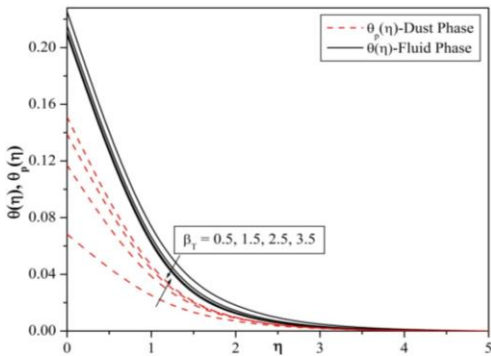

Figure 6.   Effect of fluid particle interaction parameter for temperature β_T on temperature profile.

Figures 7 and 8 explain the effect of modified Hartman number Q on velocity and temperature profile in both directions for fluid and dust phase. We noticed that the velocity profile increases and temperature profile decreases for increasing values of Q. Further, momentum boundary layer thickness is also enhanced. Physically, it is interpreted that higher values of modified Hartman number results in the development of external electric field, which consequently increases the velocity field. Impact of dimensionless parameter A on velocity distribution is illustrated in Figure 9. It is analyzed that the velocity profile and associated boundary layer thickness decrease for higher values of A. Figure 10. emblematizes the effects of the Eckert number (Ec) on temperature distribution. From this figure it is observed that the increasing values of Eckert number is to increase temperature distribution, because of the fact that heat energy is stored in the liquid due to frictional heating and this is true in both the cases.

Figure 11 illustrates the effects of the radiation parameter (Rd) on the fluid phase and dust phase temperature, and from the graph it is seen that as radiation parameter increases both phases of temperature profile increase. This is due to the fact that an increase in radiation parameter provides more heat to the fluid that causes an enhancement in the temperature and thermal boundary layer thickness. Figure 12 is sketched the temperature distributions against the Prandtl number (Pr). The decrease in thermal diffusivity is a dominant factor in Pr. This can be attributed due to diffusivity of liquid is appeared in Prandtl number that becomes weaker for higher. This figure, reveals that the temperature profile decreases for both the phases with increase in the value of Pr. Hence Prandtl number can be used to increase the rate of cooling. It is noted from all the graphs that the fluid phase is parallel to that of dust phase and also the fluid phase is higher than the dust phase. Figure 13 dissembles the change in temperature profile for different values of Biot number (Bi). Here we can see that increasing values of Biot number lead to elevated temperature and thicker thermal boundary layer thickness. This is due to the fact that the convective heat exchange at the surface leads to enhanced the thermal boundary layer thickness.
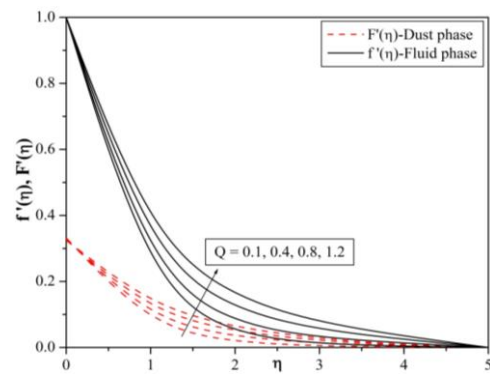

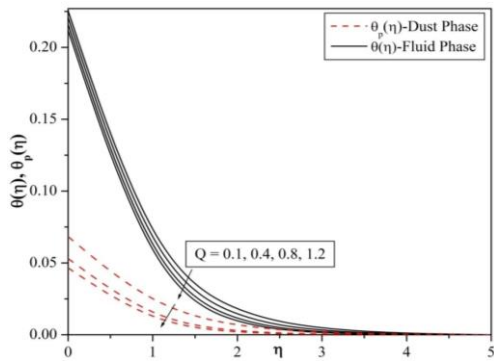Figure 7.   Effect of modified Hartman number (Q) on velocity profile.

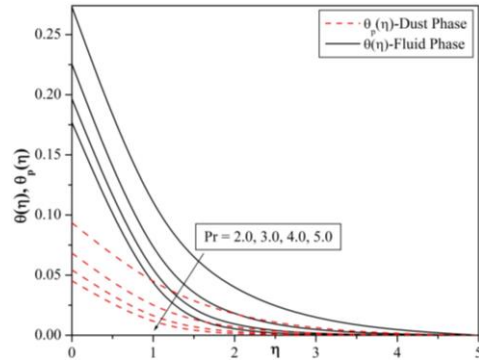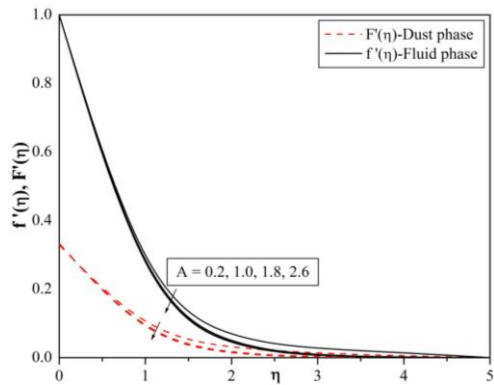Figure 8.   Effect of modified Hartman number (Q) on temperature profile.

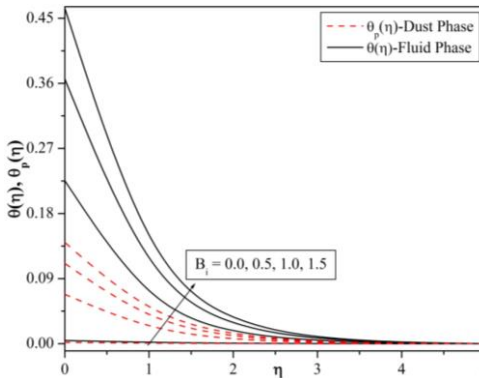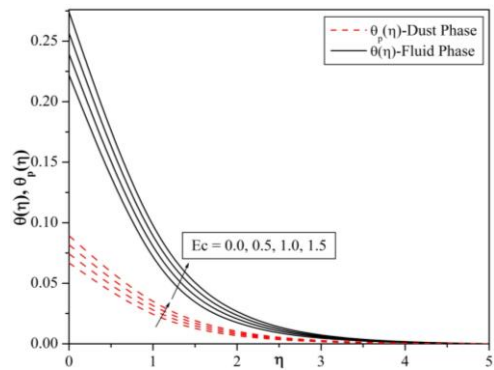Figure 9.   Effect of dimensionless parameter (A) on velocity profile.

Figure 10. Effect of Eckert number (Ec) on temperature profile.

Figure 11. Effect of radiation parameter (Rd) on temperature profile.

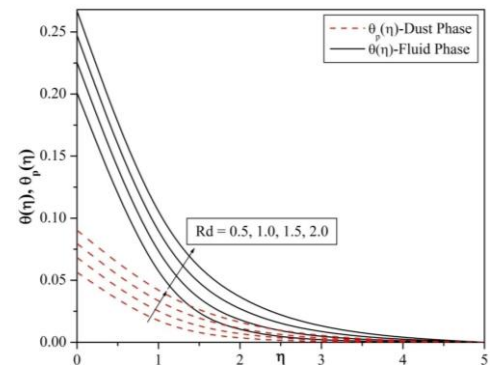Figure 12. Effect of Prandtl number (Pr) on temperature profile.

Figure 13. Effect of Biot number (B_i) on temperature profile.

We have numerically studied the effects of $kp, Ec, Pr, Q, A, Rd, \beta, \beta_T, l, B_i$ on skin friction coefficient and the local Nusselt number, which represents the heat transfer rate at the surface, and are recorded in Table 2. From this table it is clear that the magnitude of skin friction coefficient increases with increase in A, kp, β, l and decreases with increase in Q. Further, it is observed that increase in the values of Pr, Q, β_T, l increase the magnitude of local Nusselt number and also increase in the values of $A, Ec, kp\ Rd$ decreases the magnitude of local Nusselt number. The local Nusselt number increases with $Pr,$ and in consequence the heat transfer rate at the surface increases. This is due to the fact that the higher Prandtl number reduces the thermal boundary layer thickness and increases the surface heat transfer rate. Also, high Prandtl number implies more viscous fluid which tends to retard the motion.

Table 2.   Values of skin friction coefficient and Nusselt number.

Pr	Grubka and Bobba (1985)	Chen (1998)	Present study $-\theta'(0)$
0.72	1.0885	1.0885	1.0885
1.0	1.3333	1.3333	1.3333
10.0	4.7969	4.7969	4.7969

5. Conclusions

This paper investigates the MHD flow of a two-phase quiescent incompressible viscous electrically conducting dusty fluid over a Riga plate with permeable stretching body embedded in a porous medium with convective boundary condition. Similarity transformations are utilized to reduce the governing partial differential equations into a set of nonlinear ordinary differential equations. The reduced equations were numerically solved using Runge-Kutta-Fehlberg fourth-fifth order method along with shooting technique. The effects of various parameters on the flow and heat transfer are observed from the graphs, and are summarized as follows:

- ☐ Fluid phase velocity is always greater than that of the particle phase. And also fluid phase temperature is higher than the dust phase temperature.
- ☐ The effect of transverse modified Hartman number is to suppress the temperature field, which in turn causes enhancement of the velocity field.
- ☐ Velocity of fluid and dust phases decrease while the temperature of fluid and dust phases increase as permeability parameter increases.
- ☐ Temperature profile increases for Eckert number, radiation parameter, temperature ratio parameter, and Biot number, and decreases for Prandtl number and mass concentration particle parameter.
- ☐ Increase of β will decrease fluid phase velocity and increases dust phase velocity.
- ☐ Increase of β_T will decrease fluid phase and increases dust phase of temperature profile.

Acknowledgements

References

Abbas, T., Ayub, M., Bhatti, M. M., Rashidi M. M., & El-Sayed, Ali, M. (2016). Entropy generation on nanofluid flow through a horizontal Riga plate. *Entropy, 18*(6), 223, doi:10.3390/e18060223.

Abbas, T., Hayat, T., Ayub, M., Bhatti, M. M., & Alsaedi, A. (2017a). Electromagnetohydrodynamic nanofluid flow past a porous Riga plate containing gyrotactic microorganism. *Neural Computing and Applications,* 1-9. doi:10.1007/s00521-017-3165-7

Abbas, T., Bhatti, M. M., & Ayub, M. (2017b). Aiding and opposing of mixed convection Casson nanofluid flow with chemical reactions through a porous Riga plate. *Proceedings of the Institution of Mechanical Engineers, Part E: Journal of Process Mechanical Engineering, 232*(5), 519-527. doi:10.1177/0954408917719791

Ahmed, N., Khan, U., & Mohyud-Din, S. T. (2017a). Influence of thermal radiation and viscous dissipation on squeezed flow of water between Riga plates saturated with carbon nanotubes. *Colloids and Surfaces A: Physicochemical and Engineering Aspects, 522*, 389–398. doi:10.1016/j.colsurfa.2017.02.083

Ahmed, N., Khan, U., & Mohyud-Din, S. T. (2017b). Influence of nonlinear thermal radiation on the viscous flow through a deformable asymmetric porous channel: A numerical study. *Journal of Molecular Liquids, 225*, 167-173. doi:10.1016/j.molliq.2016.11.021

Ahmad, A., Asghar, S., & Afzal, S. (2016). Flow of nanofluid past a Riga plate. *Journal of Magnetism and Magnetic Materials, 402*, 44-48. doi:10.1016/j.jmmm.2015.11.043

Ayub, M., Abbas, T., & Bhatti, M. M. (2016). Inspiration of slip effects on electromagnetohydrodynamics (EMHD) nanofluid flow through a horizontal Riga plate. *European Physical Journal Plus, 131*(193). doi:10.1140/epjp/i2016-16193-4

Bhatti, M. M., Abbas, T., & Rashidi, M. M. (2016). Effects of thermal radiation and electromagnetohydrodynamic on viscous nanofluid through a Riga plate. *Multidiscipline Modeling in Materials and Structures, 12*(4), 605 – 618. doi:10.1108/MMMS-07-2016-0029

Bhatti, M. M., & Zeeshan, A. (2017). Heat and mass transfer analysis on peristaltic flow of particle fluid suspension with slip effects. *Journal of Mechanical in Medicine and Biology, 17*(2), 1750028. doi:10.1142/S0219519417500282

Chakrabarti, K.M. (1974). Note on Boundary layer in a dusty gas. *American Institute of Aeronautics and Astronautics Journal, 12*(8), 1136-1137. doi:10.2514/3.49427

Chen, C.H. (1998). Laminar mixed convection adjacent to vertical, continuously stretching sheets. *Heat Mass Trans*fer, *33*, 471–476. doi:10.1007/s002310050217

Datta, N., & Mishra, S. K. (1982). Boundary layer flow of a dusty fluid over a semi-infinite flat plate. *Acta Mechanica, 42*, 71-83. doi:10.1007/BF01176514

Farooq, M., Anjum, A., Hayat, T., & Alsaedi, A. (2016). Melting heat transfer in the flow over a variable thicked Riga plate with homogeneous-hetero geneous reactions. *Journal of Molecular Liquids, 224*, 1341–1347. doi:10.1016/j.molliq.2016.10.123

Gailitis, A., & Lielausis, O. (1961). On a possibility to reduce the hydrodynamic resistance of plate in an electrolyte. *Applied Magnetohydrodynamics, 12*, 143-146.

Gireesha, B. J., Ramesh, G. K., Abel, M. S., & Bagewadi, C. S. (2011). Boundary layer flow and heat transfer of a dusty fluid flow over a stretching sheet with non-uniform heat source/sink. *International Journal of Multiphase Flow, 37*, 977–982. doi:10.1016/j.ijmultiphaseflow.2011.03.014

Gireesha, B. J., Venkatesh, P., Shashikumar, N. S., & Prasannakumara, B. C. (2017). Boundary layer flow of dusty fluid over a permeable radiating stretching

surface embedded in a thermally stratified porous medium in the presence of uniform heat source. *Nonlinear Engineering, 6*(1), 31-41. doi:10.1515/nleng-2016-0058

Grubka, L. J., & Bobba, K. M. (1985), Heat transfer characteristics of a continuous stretching surface with variable temperature. *Journal of Heat Transfer, 107*, 248-250. doi:10.1115/1.3247387

Hayat, T., Khan, M., Imtiaz, M., & Alsaedi, A. (2017). Squeezing flow past a Riga plate with chemical reaction and convective conditions. *Journal of Molecular Liquids, 225*, 569–576. doi:10.1016/j.molliq.2016.11.089

Hayat, T., Abbas, T., Ayuba, M., Farooq, M., & Alsaedi, A. (2016). Flow of nanofluid due to convectively heated Riga plate with variable thickness. *Journal of Molecular Liquids, 222*, 2016, 854–862. doi:10.1016/j.molliq.2016.07.111

Hamid, R. A., Nazar, R., & Pop, I. (2017). Boundary layer flow of a dusty fluid over a permeable shrinking surface. *International Journal of Numerical Methods for Heat and Fluid Flow, 27*(4), 758-772. doi:10.1108/HFF-01-2016-0030

Iqbal, Z., Mehmood, Z., Azhar, E., & Maraj, E. N. (2017). Numerical investigation of nanofluidic transport of gyrotactic microorganisms submerged in water towards Riga plate. *Journal of Molecular Liquids, 234*, 296–308. doi:10.1016/j.molliq.2017.03.074

Mosayebidorcheh, S., Hatami, M., Ganji, D. D., Mosayebidorcheh, T., & Mirmohammadsadeghi, S. M. (2015). Investigation of transient MHD Couette flow and heat transfer of dusty fluid with temperature-dependent properties. *Journal of Applied Fluid Mechanics, 8*(4), 921-929. doi:10.18869/acadpub.jafm.73.238.23949

Prakash, O. M., Makinde, O. D., Kumar, D., & Dwivedi, Y. K. (2015). Heat transfer to MHD oscillatory dusty fluid flow in a channel filled with a porous medium. *Sadhana, 40*(4), 1273–1282. doi:10.1007/s12046-015-0371-9

Ramesh, G. K., Gireesha, B. J., & Gorla, R. S. R. (2015a). Boundary layer flow past a stretching sheet with fluid-particle suspension and convective boundary condition. *Heat and Mass Transfer, 51*(8), 1061-1066. doi:10.1007/s00231-014-1477-z

Ramesh, G. K., Gireesha, B. J., & Gorla, R. S. R. (2015b). Study on Sakiadis and Blasius flows of Williamson fluid with convective boundary condition. *Nonlinear Engineering, 4*(4), 215-221. doi:10.1515/nleng-2015-0020

Ramesh, G. K., Chamkha, A. J., & Gireesha, B. J. (2016). Boundary layer flow past an inclined stationary/moving flat plate with convective boundary condition. *Afrika Matematika, 27*(1-2), 87-95. doi:10.1007/s13370-015-0323-x

Ramesh, G. K., & Gireesha, B. J. (2013). Flow over a stretching sheet in a dusty fluid with radiation effect. *Journal of Heat Transfer, 35*(10), 102702. doi: 10.1115/1.4024587

Ramesh, G. K., & Gireesha, B. J. (2017a). Non-linear radiative flow of nanofluid past a moving/stationary Riga plate. *Frontiers in Heat and Mass Transfer, 9*-3. doi:10.5098/hmt.9.3

Ramesh, G. K., Roopa, G, S., Gireesha, B. J., Shehzad, S. A., & Abbasi, F. M. (2017b). An electro-magneto-hydrodynamic flow Maxwell nanoliquid past a Riga plate: A numerical study. *Journal of the Brazilian Society of Mechanical Sciences and Engineering, 39*(11), 4547-4554. doi:10.1007/s40430-017-0900-z

Saffman, P. G. (1962). On the stability of laminar flow of a dusty gas. *Journal of Fluid Mechanics, 13*, 120–128. doi:10.1017/S0022112062000555

Turkyilmazoglu, M. (2017). Magnetohydrodynamic two-phase dusty fluid flow and heat model over deforming isothermal surfaces. *Physics of Fluids, 29*, 013302. doi:10.1063/1.4965926

Vajravelu, K., & Nayfeh, J. (1992). Hydromagnetic flow of a dusty fluid over a stretching sheet. *International Journal of Nonlinear Mechanics, 27*, 937-945. doi:10.1016/0020-7462(92)90046-A